Comparison of Junction Temperature Measurement Using the TSEP Method and Optical Fiber Method in IGBT Power Modules without Silicone Gel Removal

Zhang, Kaichen; Leduc, Charles; Iannuzzo, Francesco

Published in:
PCIM 2023

Publication date:
2023

Document Version
Accepted author manuscript, peer reviewed version

pcim EUROPE

Comparison of Junction Temperature Measurement Using the TSEP Method and Optical Fiber Method in IGBT Power Modules without Silicone Gel Removal

Kaichen Zhang[1], Charles Leduc[2], Francesco Iannuzzo[1]

[1] Aalborg University, Denmark
[2] OpSens Solutions Inc., Canada

Corresponding author: Kaichen Zhang, kzh@energy.aau.dk
Speaker: Kaichen Zhang, kzh@energy.aau.dk

Abstract

The junction temperature (T_j) is a critical parameter for determining the power cycling capability of power semiconductor devices. Typically, the temperature of the chip is measured indirectly using the temperature-sensitive electrical parameter (TSEP) method or directly using classical infrared (IR) method. However, the TSEP method's suitability for measuring chip temperature in online conditions, especially for complex circuits, has not been adequately demonstrated. The direct measurement method requires removing the silicone gel, making it unsuitable for long-term operation under actual operating conditions. As an alternative approach, optical fibers have been proposed to measure the chip temperature directly through the silicone gel. This paper evaluates both the TSEP method, which measures the saturation voltage under low current, and the optical fiber method for measuring the IGBT's chip temperature under both with and without silicone gel conditions. The initial findings suggest that the presence of silicone gel affects the fiber's response and the chip's temperature distribution. However, the TSEP and optical fiber methods' results are consistent when the silicone gel is removed. The results of this study can contribute to a better understanding of the virtual junction temperature as measured by the TSEP method. Additionally, the findings highlight the advantages and disadvantages of using both the TSEP and optical fiber methods for chip temperature measurement.

1 Introduction

Power semiconductor devices with high-power density and exceptional thermal performance are in high demand for various applications, and ensuring the device's reliability is crucial for a stable power electronic system [1]. Temperature is a critical parameter that greatly influences the performance and reliability of a device. While a higher maximum junction temperature T_j tolerance can decrease the cooling system requirements, it can also increase the temperature swing and present more significant reliability challenges. Precise measurement of the junction temperature is essential for assessing the device's reliability and obtaining a realistic estimation of its lifetime. According to [2], a variation of just 10K in the power cycling condition can roughly lead to a factor of two change in the lifetime.

The junction temperature can be either indirectly estimated or directly measured. In [3] and [4], the TSEP method was applied for power cycling under high switching frequencies, but it required additional measurement circuits and careful calibration to obtain accurate T_j during operation. As noted in [5], direct measurement methods including optical and physical contact are discussed, like infrared cameras and optical fibers. In [6], a detailed description of using the infrared (IR) method for measuring the junction temperature is provided. However, the method has limitations as it requires the removal of the silicone gel, which serves as encapsulation, and applying a thin film of black paint to homogenize the surface emissivity. The two limitations will introduce the risk of operating in high-voltage applications and thermal response changes in high transient operations [7]. The use of optical fibers to measure the junction temperature directly through the silicone gel was discussed in [8] and [9], both of which noted that the locally measured temperature may not accurately represent the average chip temperature due to spatial temperature variations across the chip surface. In addition, [9] also mentioned the optical fiber's bandwidth limitations. Alternatively, a non-contact method called the thermoreflectance technique has been proposed to measure the junction temperature without the need for removing the silicone gel, as mentioned in [10]. High accuracy results were gained (sensitivity less than 1K) under the small variations of temperature conditions (low voltage).

The saturated forward voltage under low current V_{ce_sat} is a commonly used thermo-sensitive electrical parameter for the thermal characterization of commercial IGBT power modules, among many other options.The temperature obtained through V_{ce_sat} is considered to be a virtual value that reflects the average lateral temperature distribution across the IGBT chip [2]. The ability to measure junction temperature without removing the silicone gel is crucial for realistic operation of the power module. An emerging method with great potential for this application is the optical fiber approach, which offers notable advantages such as resistance to electromagnetic (EM) fields and high voltage. The method utilizes non-invasive miniature sensors that have a low thermal mass and a fast response time of around a millisecond. Moreover, the optical fiber method has a simple and rugged design that has been field-tested and can be used in modules with or without gel. It is of interest to compare the thermal response of these two methods and evaluate the impact of silicone gel on the T_j measurement.

The initial section of this paper outlines the experimental setup and the device under test (DUT). This is followed by an explanation of the optical fiber temperature measurement principle and its implementation on the power module. The paper then discusses the characterization of V_{ce_sat}. Subsequently, temperature measurements obtained using both methods under diverse test conditions are presented and analyzed. Finally, the paper concludes with a summary of the findings.

2 Experimental methods

2.1 Test bench description

The test bench (shown in Fig. 1) was constructed in a standard 19" industrial rack and comprised of two converters, namely the DUT converter and the load converter, connected in a back-to-back configuration through an inductive load and sharing the same DC-link. This design allowed for the flexibility of conducting both DC- and AC power cycling tests, and a more comprehensive description can be found in [11].

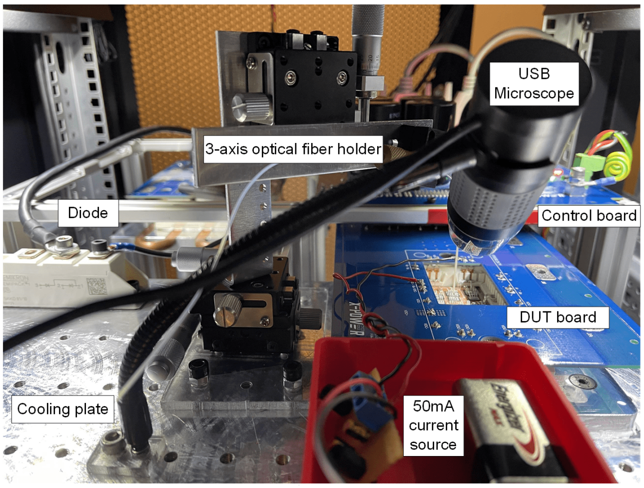

Fig. 1: Test bench for TSEP and optical fiber measurements.

To maintain a consistent case temperature on the DUT, it is mounted on a cooling plate connected to a JULABO Presto A40 chiller. A cutout is made on the top of the power module's plastic housing to allow the sensor to reach the chip surface. An optical fiber is secured on a holder comprising three micromanipulators and aluminum cantilevers, enabling pre-positioning of the sensor directly above the target measurement area. The sensor is then lowered to the chip surface by carefully adjusting the micro-manipulator in three directions. The displacement value of the sensor can be accurately controlled using the micromanipulator's scale, which has 0.01mm accuracy.

The control system consists of a host PC running NI LabVIEW and NI CompactRIO hardware. The host PC is equipped with a user-friendly graphical interface that controls the NI CompactRIO and other instruments. The NI CompactRIO utilizes several digital NI 9401 modules, both to provide the gate signals and communicate with a set of analog-to-digital converters (ADC) used for logging the on-state voltage $V_{ce(on)}$. The main PCB (control board) houses both the $V_{ce(on)}$ measurement unit and the gate unit. The $V_{ce(on)}$ is measured over the DC and Kelvin terminals of the IGBT module, with mV scale accuracy, and can be sampled per single switching period, up to 20kHz. To measure the saturated forward voltage under low current V_{ce_sat}, a constant current source circuit was added to the DUT converter, which generated a stable and adjustable constant small current using the LT3092 two-terminal integrated circuit (IC).

For the following tests, two 1200V-50A IGBT power modules (Infineon-FP50R12KT4) with similar statistical electrical characteristics were prepared, with one module having the silicone gel removed. The remaining test conditions, such as the thermal grease thickness, the torque applied to the module, and the optical fiber used for temperature measurement, were strictly controlled to be the same. The two IGBT modules instrumented with optical fibers are shown in Fig. 2.

2.2 Optical fiber measurements

In paper [12], it is explained that the optical fiber operates using the Semi-Conductor Band Gap (SCBG) fiber optic temperature sensing technology. This technique uses a gallium arsenide (GaAs) semiconductor crystal, which is transparent for wavelengths above its bandgap and opaque for wavelengths below. The crystal's bandgap spectral position varies with temperature, making it possible to measure temperature by detecting changes in light transmission. The sensor is made of a miniature GaAs crystal attached to the end of an optical fiber. Light is injected into the fiber and delivered to the GaAs crystal, where it is absorbed or reflected depending on its wavelength. The reflected light is analyzed using an optical spectrum analyzer, and the resulting spectral intensity distribution is used to determine the temperature.

The adopted OTG-PM retractable sensor from OpSens Solutions Inc. is designed to protect the sensor head during cable manipulation and test preparation when installing the fiber. Once ready for instrumentation, the sensor head can be exposed to reach the surface for monitoring. The sensor head is protected by a small but robust polyimide tubing that provides the necessary rigidity to penetrate silicon gel and position the sensor precisely on a die. The schematic cross section of the power module with optical fiber being instrumented on the chip surface is presented in Fig. 3.

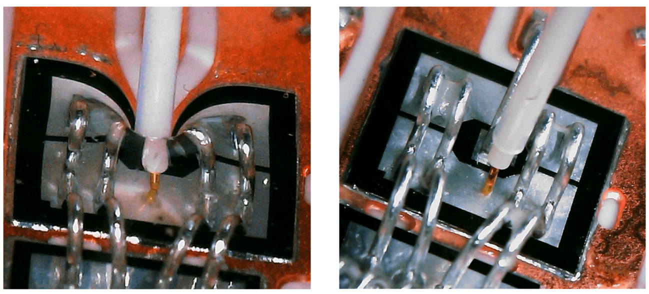

Fig. 2: IGBT modules instrumented with optical fibers (with and without gel).

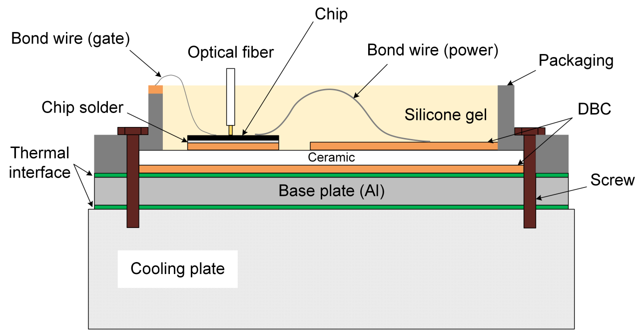

Fig. 3: Schematic view of cross section of an IGBT power module mounted on the cooling plate.

When it comes to thermal response, the OTG-PM sensor offers precise and consistent measurement results with an accuracy of ±0.8°C. Additionally, the signal conditioner utilized can achieve a sampling frequency of up to 1000Hz.

2.3 Characterization of the TSEP

This section details the calibration procedure and measurement conditions for the selected TSEP method. The power module is mounted on a cooling plate, and the chip temperature is regulated using the JULABO temperature control system, as explained in the preceding section. The saturation forward voltage under low current (V_{ce_sat}) is measured for every 10K increase in the chip temperature, ranging from 10°C to 90°C. However, because of convection and radiation heat transfers between the DUT and its surroundings at room temperature (approximately 25°C), the chip temperature is lower than that of the cooling plate. Thus the chip temperature is measured using an optical fiber. Since the entire chip is heated by the cooling plate, the measurement outcome from the optical fiber is regarded as the chip temperature at thermal equilibrium state in the calibration curves (Fig. 5). The cooling plate temperature is adjusted accordingly to ensure that the chip temperature increases linearly every 10K. To measure V_{ce_sat}, a low current supply I_c is used to power the IGBT chip (as shown in Fig. 4). In these experiments, I_c is set to 50mA, which is one-thousandth of the DUT's rated current. This low value is selected because the dissipated power in

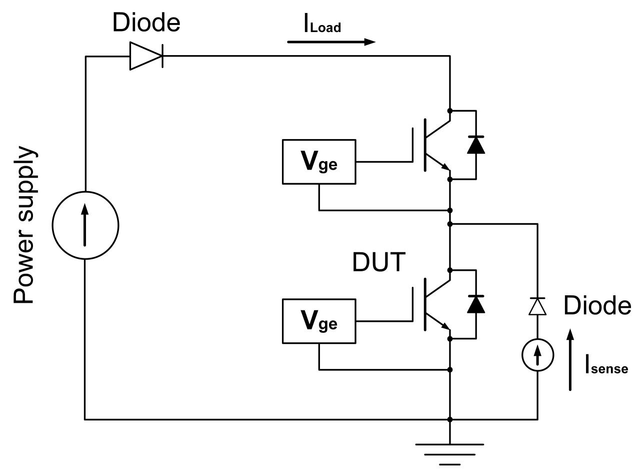

Fig. 4: Power circuit used to characterize the DUT.

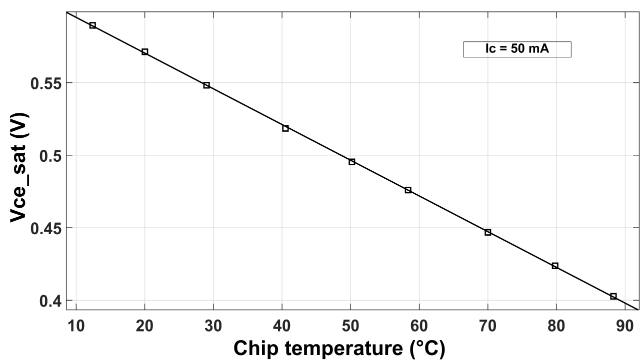

Fig. 5: Calibration curve of the temperature-dependent saturated forward voltage under low current.

the chip is very low, and continuous current injection can be applied without any self-heating of the power device. The derived calibration curve shows good linearity, negative temperature co-efficient and gives a temperature sensitivity of 2.46mV/°C.

3 Results

Three types of tests were carried out to comprehensively assess the TSEP method and the optical fiber method for measuring junction temperature. These tests were conducted under varying thermal conditions/measurement points. For all three tests, the cooling plate temperature is set to be fixed at 20°C. The gate-emitter voltage is set to 15V. The V_{ce_sat} is measured 380µs after the load current is turned off. The locations on the chip surface where the optical fiber is positioned for measurement are indicated in Fig. 2.

1) 200s thermal characterization test
2) DC power cycling test with varied on/off time
3) Multi-points temperature measurement along chip's diagonal trace

3.1 Test 1

To conduct the 200s thermal characterization test, a constant load current ranging from 5A to 30A is applied to the DUT for a duration of 200 seconds. During this test, the temperature of the target chip is measured using optical fiber method. The measurement is taken from an initial temperature of 20°C and continues until the chip has been cooled down to the cooling plate temperature again. The TSEP method is used to estimate the $T_{vj,max}$ right after the chip's active heating period, with a 380µs delay. By actively heating up the chip for a considerable time, the chip can reach thermal equilibrium state. The measured temperature is regarded as being saturated when the dT_j/dt reached 0.8°C/s.

Current	TSEP	Optical fiber	Δ
I_{load} [A]	T_{vj} [°C]	T_j [°C]	[°C]
5	22.83	23.76	0.93
10	27.27	27.88	0.61
15	31.21	32.92	1.71
20	38.12	38.89	0.77
25	44.53	45.71	1.18
30	51.93	53.51	1.58

Tab. 1: Temperature measurement results in Test 1 for DUT with gel presence.

Current	TSEP	Optical fiber	Δ
I_{load} [A]	T_{vj} [°C]	T_j [°C]	[°C]
5	23.61	23.66	0.05
10	28.07	27.29	-0.78
15	32.09	31.63	-0.46
20	37.00	36.61	-0.39
25	43.70	42.60	-1.1
30	50.85	48.60	-2.25

Tab. 2: Temperature measurement results in Test 1 for DUT without gel.

Tab.1 and Tab.2 present the test results for the DUT under with and without gel conditions, respectively. The temperature provided by the TSEP method is compared to the maximum temperature provided by the optical fiber, and the difference between the two is also calculated. It should be noted that the temperature measurements of the optical fiber between 0 and 1 ms after active heating may not be reliable due to limitations in the sampling frequency. Additionally, the temperature provided by the TSEP method represents the temperature after a cooling period of 380µs following the maximum temperature. For with gel condition, the chip temperature measurement results using both optical fiber and TSEP methods are also shown in Fig. 6.

3.2 Test 2

To conduct the DC power cycling test, a constant load current ranging from 5A to 30A is applied to the DUT for a varied on and off time. During this test, the temperature of the target chip is measured using optical fiber method. The measurement is taken from an initial temperature of 20°C and continues for a number of cycles of the DC power cycling until the maximum temperature and the temperature swing becomes stable. The TSEP method is used to estimate the $T_{vj,max}$ right after the chip's active heating period with a 380µs delay, and $T_{vj,min}$ just before the chip's active heating period to start. Both $T_{vj,max}$ and $T_{vj,min}$ are measured within the last cycle period before the DC power cycling test stopped.

Current	TSEP	Optical fiber	Swing
I_{load} [A]	$T_{vj,max/min}$ [°C]	$T_{j,max/min}$ [°C]	Δ [°C]
5	22.33 / 20.36	22.73 / 22.27	-1.51
10	26.28 / 20.85	25.58 / 24.50	-4.55
15	30.72 / 22.83	29.10 / 27.27	-6.06
20	35.65 / 23.81	32.47 / 29.76	-9.13
25	42.56 / 25.30	37.48 / 33.78	-13.56
30	49.96 / 28.26	42.73 / 37.84	-16.81

Tab. 3: Temperature measurement results with 2s on/off time in Test 2 for DUT with gel presence.

Current	TSEP	Optical fiber	Swing
I_{load} [A]	$T_{vj,max/min}$ [°C]	$T_{j,max/min}$ [°C]	Δ [°C]
5	22.71 / 21.37	23.21 / 21.79	0.08
10	26.73 / 22.27	26.49 / 23.19	-1.16
15	31.20 / 23.61	30.41 / 24.80	-1.98
20	36.56 / 24.50	34.90 / 26.69	-3.85
25	41.91 / 25.84	39.95 / 28.58	-4.7
30	47.72 / 27.18	45.80 / 30.80	-5.54

Tab. 4: Temperature measurement results with 2s on/off time in Test 2 for DUT without gel.

Tab.3 and Tab.4 present the test results for the DUT under with and without gel conditions respectively, with 2s on/off time of the DC power cycling. The maximum and minimum temperatures provided by the TSEP method is compared to the temperatures measured by the optical fiber, and the temperature swing difference between the two is also calculated. The chip temperature measurement results using both methods under 30A load current and 2s on/off time of DC power cycling are also shown in Fig. 7.

Current	TSEP	Optical fiber	Swing
I_{load} [A]	$T_{vj,max/min}$ [°C]	$T_{j,max/min}$ [°C]	Δ [°C]
5	22.33 / 19.87	22.29 / 21.56	-1.73
10	26.78 / 20.37	24.75 / 23.06	-4.72
15	30.72 / 21.35	27.67 / 24.82	-7.52
20	36.14 / 22.34	30.75 / 26.57	-9.62
25	42.56 / 23.82	34.79 / 29.16	-13.11
30	50.45 / 25.30	39.01 / 31.64	-17.78

Tab. 5: Temperature measurement results with 2s on/6s off time in Test 2 for DUT with gel presence.

Current	TSEP	Optical fiber	Swing
I_{load} [A]	$T_{vj,max/min}$ [°C]	$T_{j,max/min}$ [°C]	Δ [°C]
5	23.16 / 21.37	23.13 / 21.58	-0.24
10	28.07 / 21.82	26.31 / 22.68	-2.62
15	31.20 / 22.27	30.11 / 23.93	-2.75
20	36.11 / 23.16	34.41 / 25.37	-3.91
25	42.36 / 25.39	39.45 / 27.04	-4.56
30	48.17 / 25.84	44.95 / 28.51	-5.89

Tab. 6: Temperature measurement results with 2s on/6s off time in Test 2 for DUT without gel.

Tab.5 and Tab.6 present the test results for the DUT under with and without gel conditions respectively, with 2s on/6s off time of the DC power cycling. The maximum and minimum temperatures provided by the TSEP method is compared to the temperatures measured by the optical fiber, and the temperature swing difference between the two is also calculated.

3.3 Test 3

To depict the temperature distribution across the surface of the IGBT chip, temperature measurements were taken at eight points along the diagonal traces of the chip using optical fiber. The measurements were obtained during a DC power cycling test, with a load current of 30A and 2s on/off time. To ensure precise measurements at the selected points, the test was conducted on a silicone gel-removed module. Fig. 8 illustrates the locations of the eight points (P0-P7) on the surface of the chip.

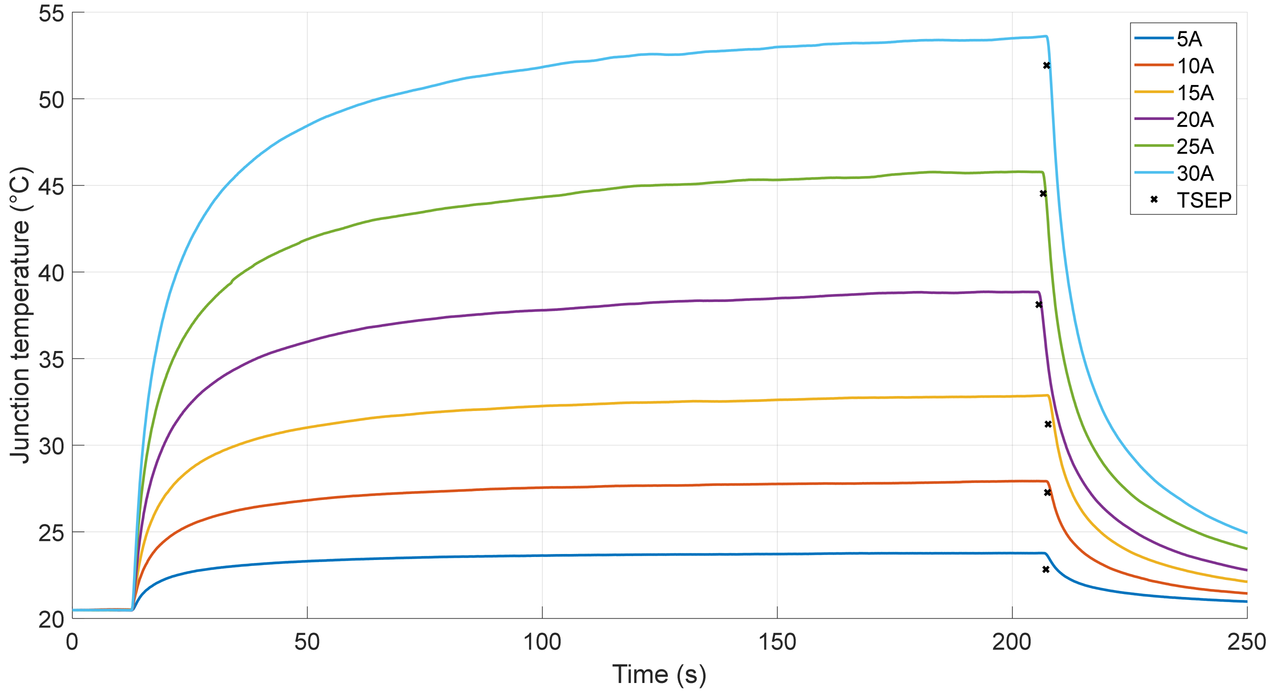

(a)

Fig. 6: Temperature measurement results under varied load currents in Test 1 for DUT with gel presence.

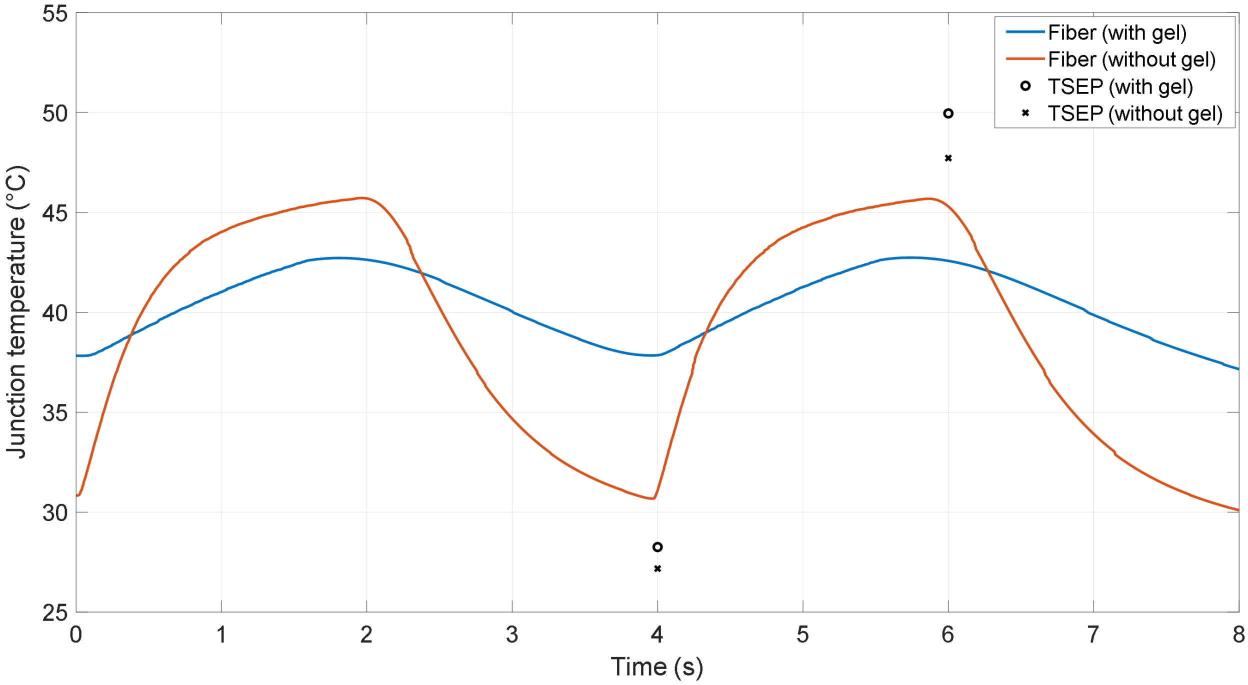

(a)

Fig. 7: Temperature measurement results under 30A load current in Test 2 with 2s on/off time.

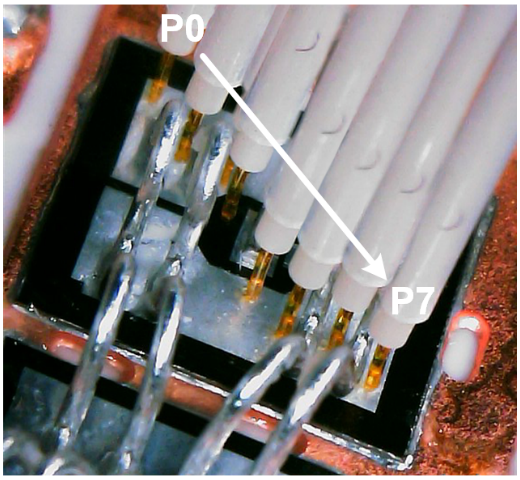

Fig. 8: Temperature measurement points (P0-P7) in Test 3 for DUT without gel.

Point	$T_{j,max}$ [°C]	$T_{j,min}$ [°C]	Swing [°C]
P0	41.08	30.07	11.01
P1	47.66	30.88	16.78
P2	47.77	30.68	17.09
P3	48.34	31.01	17.33
P4	47.13	30.89	16.24
P5	49.21	31.22	17.99
P6	49.76	31.74	18.02
P7	43.75	30.43	13.32
TSEP	47.72	27.18	20.54

Tab. 7: Temperature measurement results in Test 3 for DUT without gel.

Tab.7 presents the temperature measurements obtained from the eight points during Test 3. Additionally, the TSEP result under the same test conditions is provided as a reference.

4 Discussions and Conclusions

The results demonstrate that higher temperatures are observed when silicone gel is present, across different test conditions. This is evident in both Test 1, as seen from the TSEP and optical fiber methods, and Test 2, as demonstrated by the TSEP method. However, the trend is not as apparent in the results obtained using the optical fiber method in Test 2. This can be deduced that the silicone gel's existence slows down the optical fiber's thermal response, no matter how fast the optical fiber's original thermal response time is. The difference in chip temperature between the conditions with and without gel can be explained as follows. When there is no gel, air allows for poor heat transfer, but it prevents thermal energy from being stored near the chips. However, in the presence of silicone gel, which has a low specific heat capacity, heat can gradually accumulate in a thin layer at the interface between the gel and the materials in contact just below during long operations. There is a difference in the measurements obtained by the TSEP and optical fiber methods, which can be attributed to measurement errors. The TSEP method measures temperature with a delay of several hundreds of µs, while the optical fiber method may give a fuzzy region in its results between 0-1 ms due to limitations in the sampling frequency, in addition to their intrinsic accuracy error. However, the main reason for most of the difference can be found in Test 3, where the TSEP provides an averaged virtual junction temperature, while the optical fiber measures the temperature at specific points on the chip surface. In general, both the optical fiber and TSEP methods have their own advantages and disadvantages. The optical fiber method can provide a precise and accurate measurement result with high spatial resolution, but its response time is slowed down when measuring temperature in the presence of silicone gel. On the other hand, the TSEP method shows fast response time with relatively good accuracy, but requires a complex measurement circuit that may affect the normal operation of the DUT during online measurements. Moreover, the electrical parameters used in the TSEP method may be influenced by the degradation and aging of power modules. Further research is needed to investigate the impact of silicone gel on optical fiber measurement results and to find possible compensation methods for online junction temperature measurement using optical fibers.

5 Acknowledgments

This work is supported by the X-POWER project from Danish Agency for Science and Higher Education. The authors would like to thank OpSens Solutions Inc. for their support in the optical fiber setup.

References

[1] H. Wang, M. Liserre, and F. Blaabjerg, "Toward reliable power electronics: Challenges, design tools, and opportunities," *IEEE Industrial Electronics Magazine*, vol. 7, no. 2, pp. 17–26, 2013.

[2] F. Nehr and U. Scheuermann, “Consequences of temperature imbalance for the interpretation of virtual junction temperature provided by the VCE(T)-method,” in *PCIM Europe 2022; International Exhibition and Conference for Power Electronics, Intelligent Motion, Renewable Energy and Energy Management*, 2022, pp. 1–8.

[3] J. Brandelero, J. Ewanchuk, and S. Mollov, “Online junction temperature measurements for power cycling power modules with high switching frequencies,” in *2016 28th International Symposium on Power Semiconductor Devices and ICs (ISPSD)*, 2016, pp. 191–194.

[4] U. Choi, F. Blaabjerg, F. Iannuzzo, and S. Jørgensen, “Junction temperature estimation method for a 600V, 30A IGBT module during converter operation,” *Microelectronics Reliability*, vol. 55, no. 9, pp. 2022–2026, 2015, Proceedings of the 26th European Symposium on Reliability of Electron Devices, Failure Physics and Analysis.

[5] N. Baker, M. Liserre, L. Dupont, and Y. Avenas, “Improved reliability of power modules: A review of online junction temperature measurement methods,” *IEEE Industrial Electronics Magazine*, vol. 8, no. 3, pp. 17–27, 2014.

[6] L. Dupont, Y. Avenas, and P.-O. Jeannin, “Comparison of junction temperature evaluations in a power IGBT module using an IR camera and three thermo-sensitive electrical parameters,” in *2012 Twenty-Seventh Annual IEEE Applied Power Electronics Conference and Exposition (APEC)*, 2012, pp. 182–189.

[7] G. Ptaszek, P. Cawley, D. Almond, and S. Pickering, “Transient thermography testing of unpainted thermal barrier coating (TBC) systems,” *NDT E International*, vol. 59, pp. 48–56, 2013.

[8] V. Smet, F. Forest, J.-J. Huselstein, F. Richardeau, Z. Khatir, *et al.*, “Ageing and failure modes of IGBT modules in high-temperature power cycling,” *IEEE Transactions on Industrial Electronics*, vol. 58, no. 10, pp. 4931–4941, 2011.

[9] M. Piton, B. Chauchat, and J. Servière, “Implementation of direct chip junction temperature measurement in high power IGBT module in operation — railway traction converter,” *Microelectronics Reliability*, vol. 88-90, Sep. 2018.

[10] Y. Metayrek, T. Kociniewski, and Z. Khatir, “Thermal mapping at the cell level of chips in power modules through the silicone gel using thermoreflectance,” *Microelectronics Reliability*, vol. 105, p. 113 563, 2020.

[11] K. Zhang, M. B. Fogsgaard, and F. Iannuzzo, “Intelligent DC- and AC power-cycling platform for power electronic components,” in *2022 IEEE Applied Power Electronics Conference and Exposition (APEC)*, 2022, pp. 307–311.

[12] C. Leduc, G. Duplain, and J.-R. St-Laurent, “Improving power electronics reliability with fiber optics sensors,” in *2022 IEEE 13th International Symposium on Power Electronics for Distributed Generation Systems (PEDG)*, 2022, pp. 1–7.